ISBN: 978-3-95450-234-9 ISSN: 2673-5504 doi:10.18429/JACoW-SRF2023-MOPMB020

A COMPREHENSIVE PICTURE OF HYDRIDE FORMATION AND DISSIPATION*

N. S. Sitaraman†, T. A. Arias, M. U. Liepe
Department of Physics, Cornell University, Ithaca, NY, USA
A. Harbick‡, M. Transtrum
Department of Physics and Astronomy, Brigham Young University, Provo, UT, USA

Abstract

Research linking surface hydrides to Q-disease, and the subsequent development of methods to eliminate surface hydrides, is one of the great successes of SRF cavity R&D. We use time-dependent Ginzburg-Landau to extend the theory of hydride dissipation to sub-surface hydrides. Just as surface hydrides cause Q-disease behavior, we show that sub-surface hydrides cause high-field Q-slope (HFQS) behavior. We find that the abrupt onset of HFQS is due to a transition from a vortex-free state to a vortex-penetration state. We show that controlling hydride size and depth through impurity doping can eliminate HFQS.

INTRODUCTION

Hydride formation occurs at cryogenic temperatures in a process analogous to familiar water vapor condensation, where the high-entropy "gas" of interstitial hydrogen minimizes its free energy by organizing into "droplets," i.e. hydride crystals. These crystals can accurately be described as low-energy ordered configurations of interstitial hydrogen with some accompanying distortion of the niobium lattice [1]. In general, the physics of droplet formation is not trivial because there is a surface energy associated with the droplets which competes with the volume energy associated with the bulk phase transition. The volume energy grows with the cube of hydride radius while the surface energy grows with the square of hydride radius. Thus, for given conditions of hydrogen chemical potential and temperature, there is a "critical" droplet radius above which hydride crystals are stable and below which they are unstable [2]. The fact that sub-critical droplets are unstable means that the hydrogen atoms must form a super-critical droplet purely by statistical chance, so that there is a free energy barrier to hydride precipitation which is potentially much larger than the thermal energy scale. The rate of droplet nucleation depends exponentially on this ratio and so can potentially be many orders of magnitude slower than the hopping rate of impurities.

The free energy barrier to hydride precipitation depends on the size of the critical droplet, which generally varies throughout a macroscopic sample. Of particular interest are the places where the critical droplet size and corresponding free energy barrier are small enough that hydrides can form quickly relative to the typical timescale (minutes) of cavity cooldown —we will call these places "nucleation sites." Many material defects can potentially affect critical droplet size, including interstitial impurities, as well as more complex defects, such as impurity-vacancy complexes, dislocations and grain boundaries, that we will not describe in detail here. Impurities are of particular interest because their near-surface concentrations can be altered through low-temperature baking, and because first-principles calculations have previously shown that they create low-energy trap sites for hydrogen, potentially encouraging hydride nucleation [3]

We present a new theory for the important physical effects of low-temperature bakes, how they improve cavity performance, and what can be done to further improve high-field quality factors. We use time-dependent Ginzburg-Landau theory to calculate dissipation from sub-surface nanohydrides, finding excellent agreement with experimentally-observed high-field Q-slope (HFQS) behavior [4] and a clear relationship between hydride size and position and HFQS onset field. We argue that increasing the concentration of hydride nucleation sites by impurity doping effectively decreases the typical size of hydrides, delaying the onset of HFQS and improving cavity performance. Our results lend additional credibility to the idea that low-temperature bakes affect high-field cavity behavior by controlling nanohydride formation.

METHODS

The Time-Dependent Ginzburg-Landau Equations

Ginzburg-Landau (GL) theory is one of the oldest theories of superconductivity, and it remains relevant today owing to its relative simplicity and direct physical insights into the electrodynamic response of superconductors under static applied fields and currents[5]. The *time-dependent* Ginzburg-Landau (TDGL) equations were originally proposed by Schmid[6] in 1966 and Gor'kov and Eliashberg[7] derived them rigorously from BCS theory later in 1968. The TDGL equations (in Gaussian units) are given by:

* This work was supported by the U.S. National Science Foundation under Award PHY-1549132, the Center for Bright Beams.
† nss87@cornell.edu, these authors contributed equally
‡ aidenharbick@gmail.com, these authors contributed equally

ISBN: 978-3-95450-234-9 ISSN: 2673-5504 doi:10.18429/JACoW-SRF2023-MOPMB020

$$\Gamma\left(\frac{\partial\psi}{\partial t}+\frac{ie_s\phi}{\hbar}\psi\right)+\frac{1}{2m_s}\left(-i\hbar\nabla-\frac{e_s}{c}\mathbf{A}\right)^2\psi+\alpha\psi+\beta|\psi|^2\psi=0 \tag{1}$$

$$\frac{4\pi\sigma_n}{c}\left(\frac{1}{c}\frac{\partial\mathbf{A}}{\partial t}+\nabla\phi\right)+\nabla\times\nabla\times\mathbf{A}-\frac{2\pi ie_s\hbar}{m_sc}\left(\psi^*\nabla\psi-\psi\nabla\psi^*\right)+\frac{4\pi e_s^2}{m_sc^2}|\psi|^2\mathbf{A}=0. \tag{2}$$

These equations are solved for the superconducting order parameter, ψ, and the magnetic vector potential, $\mathbf{A}$. The magnitude squared of ψ roughly corresponds to the density of superconducting electrons. Additionally, ϕ is the scalar potential, σ_n is the normal conductivity, Γ is the phenomenological rate of relaxation of ψ, and $e_s = 2e$ and $m_s = 2m_e$ are the total charge and total effective mass of a Cooper pair, respectively. The TDGL equations are subject to boundary conditions

$$\left(i\hbar\nabla\psi+\frac{e_s}{c}\mathbf{A}\psi\right)\cdot\mathbf{n}=0 \tag{3}$$

$$(\nabla\times\mathbf{A})\times\mathbf{n}=\mathbf{H}_a\times\mathbf{n} \tag{4}$$

$$\left(\nabla\phi+\frac{1}{c}\frac{\partial\mathbf{A}}{\partial t}\right)\cdot\mathbf{n}=0, \tag{5}$$

where $\mathbf{n}$ is the outward normal vector to the boundary surface and $\mathbf{H}_a$ is the applied magnetic field. Equation 3 ensures no current will flow out of the superconducting domain, and noting that $E = -\nabla\phi - \frac{1}{c}\frac{\partial\mathbf{A}}{\partial t}$, equations 4 and 5 are typical electromagnetic interface conditions with an applied magnetic field.

The parameters α, β, and Γ were originally introduced into the theory as phenomenological, temperature-dependent constants[8], but they can also be derived from microscopic theory using the time-dependent Gor'Kov equations[7]. A useful consequence of this derivation is that these parameters can be directly related to experimentally observable properties of the material in question. The material dependencies we use are given by Kopnin[9]:

$$\alpha(\nu(0),T_c,T)\approx\nu(0)\left(1-\frac{T}{T_c}\right) \tag{6}$$

$$\beta(\nu(0),T_c,T)\approx\frac{7\zeta(3)\nu(0)}{8\pi^2T_c^2} \tag{7}$$

$$\Gamma(\nu(0),T_c)=\frac{\nu(0)\pi\hbar}{8T_c}, \tag{8}$$

where $\nu(0)$ is the density of states at the Fermi-level, T_c is the critical temperature, T is the temperature, and $\zeta(x)$ is the Riemann zeta function. It is also worth noting that $\alpha < 0$ corresponds to the superconducting state whereas $\alpha \geq 0$ corresponds to the normal state; β is strictly positive.

The TDGL equations are not without their limitations. They are only valid for gapless superconductivity, as gapped superconductors have a singularity in their density of states which prevents expansions in powers of the energy gap[10]. Additionally, the equations are only quantitatively valid near the critical temperature. The first of these conditions can be avoided with the use of a generalized version of TDGL first proposed by Kramer and Watts-Tobin[11]. Future work could include the use of this generalized TDGL; however, it should be noted that Proslier et al.[12] observed a broadening in the density of states due to Nb oxides leading to a gapless superconducting surface layer in certain Nb SRF cavities. Gurevich and Kubo[13, 14] later showed that under typical SRF operating conditions and material compositions, there is a generic broadening of the density of states and lowering of the gap, which further justifies the use of TDGL for SRF applications.

Dissipation in TDGL

When simulating SRF materials, dissipation is often a physical quantity of interest. Under TDGL, a formula for dissipation can be derived by considering the time derivative of the free energy and the free energy current flux density. A more detailed derivation is found in Kopnin[9], but we quote the final result for the dissipation W here:

$$W=2\Gamma\left|\left(\frac{\partial\psi}{\partial t}+\frac{ie_s\phi\psi}{\hbar}\right)\right|^2+\sigma_n\mathbf{E}^2. \tag{9}$$

The first term above corresponds to the superconducting dissipation arising from the relaxation of the order parameter. The second term is the dissipation of normal currents which are largest near the surface where magnetic field can still appreciably penetrate.

It is worth considering how this expression for the dissipation is related to existing theories of RF power loss and surface resistance. The first term in Equation 9 is associated with the dissipation due to the rate of change of ψ in the vortex state. In the meissner state this term is small, but it becomes large in the mixed state when there is vortex motion. A dissipation of this form is similar to that proposed by Tinkham[15], who suggested the vortex dissipation should be proportional to $\left(\frac{\partial\psi}{\partial t}\right)^2$. The additional term within the parenthesis in Equation 9 is a result of the gauge invariance of TDGL. The second term in Equation 9 can be directly related to the phenomenological "two-fluid model," which was first proposed by Gorter and Casimir[16] in 1934 and was applied by London[17] later that year to calculate the power loss of a superconductor. The two-fluid model approximates the electrons of the system as consisting of two non-interacting 'fluids': the superconducting electrons, in the form of cooper pairs which carry lossless supercurrent, and the normal electrons, which exist as thermally excited quasiparticles that produce typical dissipative currents. Under the two-fluid model, the normal fluid losses produce dissipation[18, 19] $P \propto \sigma_n E^2$, which is identical to the second term of the

ISBN: 978-3-95450-234-9 ISSN: 2673-5504 doi:10.18429/JACoW-SRF2023-MOPMB020

TDGL expression for superconducting dissipation. For AC applied currents, the electric field is proportional to the frequency and magnetic field, $E \propto \omega H$, meaning that overall the power loss will be of the form $P \sim \omega^2 H^2$. In the low frequency and low field limit, the well known "BCS resistance" originally calculated by Mattis and Bardeen[20] as well as independently by Abrikosov, Gor'Kov, and Khalatnikov[21] reduces to the form[13, 22]

$$R_{bcs} \simeq \frac{\omega^2}{T} e^{\frac{-\Delta}{k_B T}}$$

where $\Delta = 1.76 k_B T_c$ is the superconducting energy gap[9]. Noting that RF power loss is given by

$$P \simeq R \int H^2,$$

where R is the surface resistance, we can see that our calculated expression for the normal state dissipation is in good agreement with the BCS prediction in the low frequency and field limit. It is important to note, however, that the BCS predictions outside of this regime will likely do a better job of matching experiment.

Determining Microscopic Properties

Using the framework from the previous section, the TDGL equations are capable of capturing materials features present in realistic samples and cavities. In particular, this method provides an effective approach to model defects in a dynamical environment. Experimental data can be used to determine suitable values for α and β in the bulk of materials, but a significant advantage of our framework is the connection between these TDGL parameters and well-defined, microscopic quantities such as $\nu(0)$ and T_c. These measurable quantities can also be calculated using density-functional theory (DFT) which provides the advantage and capability of capturing spatial variations of these parameters that can fluctuate on a microscopic level. Local densities of states are straightforward to compute in DFT, providing local values for $\nu(0)$ and superconducting quantities such as T_c are calculated by applying Eliashberg theory within a DFT framework and directly calculating electron-phonon coupling from first principles. Further information regarding the details and results from the DFT calculations used here can be read in Ref. [23].

Finite Element Formulation

In this paper we solve the TDGL equations in 3D via a finite element method proposed by Gao[24]. We choose the popular temporal gauge which sets the scalar potential $\phi = 0$ (see Du[25] for a more detailed overview of gauge choices for TDGL). All computations in this paper were done using the open source software FEniCS[26].

RESULTS

The distribution of nucleation sites can greatly influence the size and location of hydrides. To illustrate this, we consider a simple classical model of hydride nucleation, which begins with a uniform concentration of free hydrogen interstitial impurities and an exponential profile of nucleation sites. In this model, hydrogen atoms freeze if they arrive at a site adjacent to a nucleation site, or if they arrive at a site adjacent to a frozen hydrogen interstitial. To model a niobium surface which has been impurity-doped to some degree, we take the concentration of nucleation sites to be simply proportional to the concentration of impurities. Figure 1 shows the results of this model. We find that a shallow doping depth results in large hydrides near the surface, while a deeper doping depth results in much smaller hydrides near the surface. Generally, hydride size is inversely proportional to nucleation site concentration, as expected.

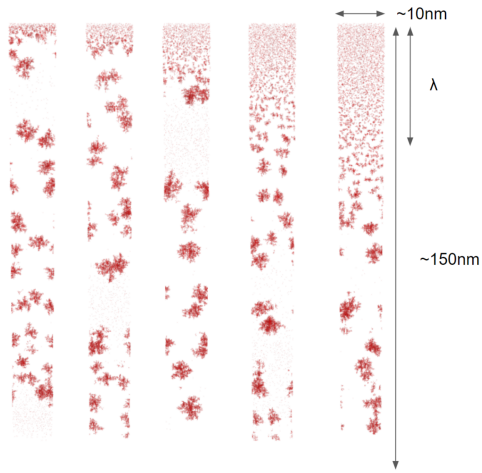

Figure 1: Qualitative simulations of hydride nucleation for different exponential nucleation site distributions, from shallowest (left) to deepest (right).

To see whether an impurity-mediated change in nucleation site distribution can accurately explain the effect of low-T bakes on cavity performance, we use density-functional theory to calculate material properties of hydrides [23], and then we perform time-dependent Ginzburg-Landau (TDGL) theory simulations of hydride dissipation, the results of which are detailed in this section.

We find that hydrides have a low-field state in which they dissipate more energy per unit volume than the superconducting niobium, resulting in a lower low-field quality factor Q_0. This dissipation is simply the result of normal currents of Bogoliubov quasiparticles moving through a material of finite resistivity; it does not cause any noticeable Q-slope, and for realistic hydride concentrations the overall effect on dissipation is small.

We find that hydrides have a fundamentally different high-field state in which a more complicated dissipation mechanism occurs, involving penetration of flux vortices. The transition from the low-field state to the high-field state is associated with an abrupt increase in calculated energy dissipation, or an abrupt onset of Q-slope, at a critical value of the peak magnetic field. Vortex penetration occurs because the proximity-coupling effect affects the superconducting properties of the niobium surface above a sub-surface hy-

ISBN: 978-3-95450-234-9 ISSN: 2673-5504 doi:10.18429/JACoW-SRF2023-MOPMB020

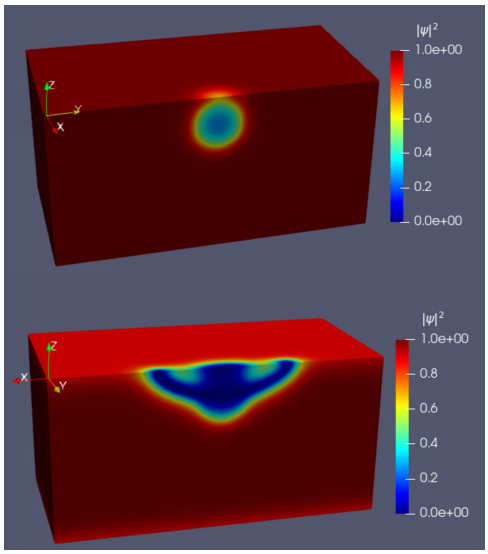

Figure 2: Simulations of superconducting order parameter at zero field (top), showing a weak spot at the surface, and at high field (bottom) showing flux vortex entry.

dride. This creates a weak spot where flux vortex penetration can occur at fields significantly below the superheating field (Fig. 2).

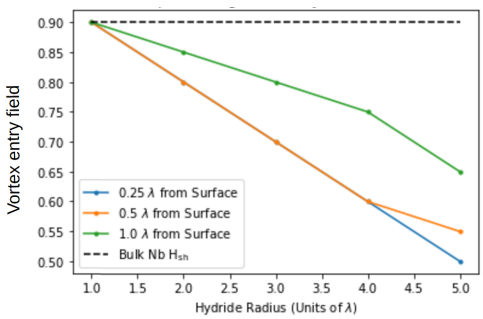

Figure 3: Calculated vortex entry field as a function of hydride radius for hydrides at different depths.

Dissipation from hydrides in the vortex state, unlike dissipation from hydrides in the non-vortex state, is highly field-dependent. This can be explained in part by the fact that, as the field increases beyond the critical field for vortex entry into the hydride, the fraction of the RF cycle at or above this critical field increases rapidly, thus increasing the length of time per cycle that vortex-related dissipation occurs. Additionally, we find that the number of vortices entering a hydride increases with increasing field, further increasing dissipation. Together, these effects result in a steep Q-slope beyond the critical field for vortex entry.

Hydride size and proximity to the surface play a crucial role in determining the critical field for vortex entry into the hydride (Fig. 3). Therefore, the distribution of hydrides has an important effect on cavity quality factor at high fields, specifically by altering the adverse high-field Q-slope (HFQS) behavior. Our results indicate that modest changes

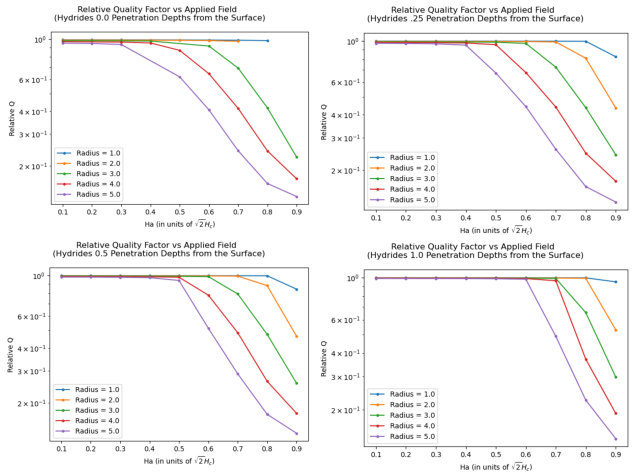

Figure 4: Calculated hydride dissipation as a function of field for hydrides at different depths (from shallowest at upper left to deepest at lower right) and of different sizes (different colored lines in each plot).

to the characteristic size of near-surface hydrides can explain experimentally observed changes in the onset field of the high-field Q-slope (Fig. 4) [4].

CONCLUSIONS

In general, we expect that in a realistic surface with a distribution of hydride sizes and positions there will be a somewhat gradual transition from low-field behavior with little to no Q-slope to high-field behavior with a steep Q-slope at fields where "typical" near-surface hydrides transition into the vortex state. This is in excellent agreement with experimental Q-slope measurements in low-T baked cavities, as well as measurements in "clean" cavities which do not undergo baking and have very low impurity content. Measurements on cavities with very low impurity content, or with a relatively short exponential doping profile, clearly show a low-field state with little Q-slope followed by a distinct HFQS state. As other researchers have pointed out, the onset field of HFQS is directly related to impurity doping [27]. The observed trend is consistent with our model if the characteristic size of hydrides is indeed inversely proportional to impurity concentration. We emphasize that this is subtly different from the mechanism researchers had previously proposed, in which impurities trap near-surface hydrogen and prevent hydride formation. While it is unlikely that impurities can trap enough hydrogen to completely eliminate hydride formation, our results show that it is not necessary to entirely eliminate hydrides in order to eliminate the HFQS. It is only necessary to eliminate large hydrides which transition into the vortex state significantly below the niobium superheating field. Therefore, counter-intuitively, creating more hydride nucleation sites near the surface can have a beneficial effect by decreasing the characteristic size of hydrides.

ISBN: 978-3-95450-234-9 ISSN: 2673-5504 doi:10.18429/JACoW-SRF2023-MOPMB020

REFERENCES

[1] J. Hauck, "Ordering of hydrogen in niobium hydride phases," *Acta Crystallogr., Sect. A: Cryst. Phys., Diffr., Theor. Gen. Crystallogr.*, vol. 33, pp. 208–211, 1977. doi:10.1107/S0567739477000424

[2] J. S. Langer, "Statistical theory of the decay of metastable states," *Ann. Phys.*, vol. 54, pp. 258–275, 1969. doi:10.1016/0003-4916(69)90153-5

[3] D. C. Ford, L. D. Cooley, and D. N. Seidman, "Suppression of Hydride Precipitates in Niobium Superconducting Radio-Frequency Cavities," Tech. Rep. FERMILAB-PUB-12-516-TD, 2013.

[4] M. Checchin and A. Grassellino, "High-field Q-slope mitigation due to impurity profile in superconducting radio-frequency cavities," *Appl. Phys. Lett.*, vol. 117, p. 032 601, 2020. doi:10.1063/5.0013698

[5] V. L. Ginzburg and L. D. Landau, "On the Theory of Superconductivity," in *On Superconductivity and Superfluidity: A Scientific Autobiography*. 2009, pp. 113–137. doi:10.1007/978-3-540-68008-6_4

[6] A. Schmid, "A time dependent Ginzburg-Landau equation and its application to the problem of resistivity in the mixed state," *Phys. Kondens. Mater.*, vol. 5, p. 302, 1966. doi:10.1007/BF02422669

[7] L. Gor'Kov and G. Eliashberg, "Generalization of the Ginzburg-Landau equations for non-stationary problems in the case of alloys with paramagnetic impurities," *Sov. Phys. JETP*, vol. 27, p. 328, 1968.

[8] Q. Du, M. D. Gunzburger, and J. S. Peterson, "Analysis and Approximation of the Ginzburg–Landau Model of Superconductivity," *SIAM Rev.*, vol. 34, pp. 54–81, 1992. doi:10.1137/1034003

[9] N. Kopnin, *Theory of nonequilibrium superconductivity*. Oxford University Press, 2001, vol. 110.

[10] M. Tinkham, *Introduction to Superconductivity*. Courier Corporation, 2004.

[11] L. Kramer and R. J. Watts-Tobin, "Theory of Dissipative Current-Carrying States in Superconducting Filaments," *Phys. Rev. Lett.*, vol. 40, pp. 1041–1044, 1978. doi:10.1103/PhysRevLett.40.1041

[12] T. Proslier *et al.*, "Tunneling study of cavity grade Nb: Possible magnetic scattering at the surface," *Appl. Phys. Lett.*, vol. 92, p. 212 505, 2008. doi:10.1063/1.2913764

[13] A. Gurevich and T. Kubo, "Surface impedance and optimum surface resistance of a superconductor with an imperfect surface," *Phys. Rev. B*, vol. 96, p. 184 515, 2017. doi:10.1103/PhysRevB.96.184515

[14] T. Kubo and A. Gurevich, "Field-dependent nonlinear surface resistance and its optimization by surface nanostructuring in superconductors," *Phys. Rev. B*, vol. 100, p. 064 522, 2019. doi:10.1103/PhysRevB.100.064522

[15] M. Tinkham, "Viscous Flow of Flux in Type-ii Superconductors," *Phys. Rev. Lett.*, vol. 13, pp. 804–807, 1964. doi:10.1103/PhysRevLett.13.804

[16] C. J. Gorter and H. Casimir, "On supraconductivity I," *Physica*, vol. 1, pp. 306–320, 1934. doi:10.1016/S0031-8914(34)90037-9

[17] H. London, "Production of heat in supraconductors by alternating currents," *Nature*, vol. 133, pp. 497–498, 1934. doi:10.1038/133497b0

[18] J. Halbritter, "On surface resistance of superconductors," *Z. Med. Phys.*, vol. 266, pp. 209–217, 1974. doi:10.1007/BF01668842

[19] J. Turneaure, J. Halbritter, and H. Schwettman, "The surface impedance of superconductors and normal conductors: The Mattis-Bardeen theory," *J. Supercond.*, vol. 4, pp. 341–355, 1991. doi:10.1007/BF00618215

[20] D. C. Mattis and J. Bardeen, "Theory of the anomalous skin effect in normal and superconducting metals," *Phys. Rev.*, vol. 111, p. 412, 1958. doi:10.1103/PhysRev.111.412

[21] A. Abrikosov, L. Gor'Kov, and I. Khalatnikov, "A superconductor in a high frequency field," *Sov. Phys. JETP*, vol. 35, p. 182, 1959.

[22] A. Gurevich, "Theory of RF superconductivity for resonant cavities," *Supercond. Sci. Technol.*, vol. 30, p. 034 004, 2017. doi:10.1088/1361-6668/30/3/034004

[23] N. S. Sitaraman, "Theory Work on SRF Materials," Ph.D. dissertation, Cornell University, 2022. doi:10.7298/mc9b-ty97

[24] H. Gao and W. Sun, "A New Mixed Formulation and Efficient Numerical Solution of Ginzburg–Landau Equations Under the Temporal Gauge," *SIAM J. Sci. Comput.*, vol. 38, A1339–A1357, 2016. doi:10.1137/15M1022744

[25] Q. Du, "Global existence and uniqueness of solutions of the time-dependent ginzburg-landau model for superconductivity," *Appl. Anal.*, vol. 53, pp. 1–17, 1994. doi:10.1080/00036819408840240

[26] M. S. Alnæs *et al.*, "The FEniCS project version 1.5," *Archive of Numerical Software*, vol. 3, pp. 9–23, 2015. doi:10.11588/ans.2015.100.20553

[27] D. Bafia *et al.*, "R&D Towards High Gradient CW SRF Cavities," in *Proc. LINAC'22*, Liverpool, UK, 2022, pp. 295–299. doi:10.18429/JACoW-LINAC2022-TU1AA03